

# Mesenchymal Stem Cell-Conditioned Medium Protects Hippocampal Neurons From Radiation Damage by Suppressing Oxidative Stress and Apoptosis

Dose-Response:  
An International Journal  
January-March 2021:1-10  
© The Author(s) 2021  
Article reuse guidelines:  
sagepub.com/journals-permissions  
DOI: 10.1177/1559325820984944  
journals.sagepub.com/home/dos



Yue Huang<sup>1</sup> , Xiaolong Mei<sup>2</sup>, Weishi Jiang<sup>1</sup>, Hui Zhao<sup>3</sup>, Zhenyu Yan<sup>4</sup>,  
Haixia Zhang<sup>4</sup>, Ying Liu<sup>1</sup>, Xia Hu<sup>1</sup>, Jingyi Zhang<sup>1</sup>, Wenshuo Peng<sup>1</sup>, Jing Zhang<sup>5,6,7,8</sup>,  
Qingling Qi<sup>9</sup>, and Naiyao Chen<sup>4</sup>

## Abstract

**Objective:** To investigate the effects of mesenchymal stem cell-conditioned medium (MSC-CM) on radiation-induced oxidative stress, survival and apoptosis in hippocampal neurons.

**Methods:** The following groups were defined: Control, radiation treatment (RT), RT+MSC-CM, MSC-CM, RT + N-Acetylcysteine (RT+NAC), and RT + MSC-CM + PI3 K inhibitor (LY294002). A cell Counting Kit-8 (CKK-8) was used to measure cell proliferation. Apoptosis was examined by AnnexinV/PI flow cytometric analyses. Intracellular reactive oxygen species (ROS) were detected by DCFH-DA. Intracellular glutathione (GSH), malondialdehyde (MDA) content, and superoxide dismutase (SOD) activity were detected by colorimetric assays. Protein levels of  $\gamma$ -H2AX, PI3K-AKT, P53, cleaved caspase-3, Bax, and Bcl-2 were analyzed by Western blotting.

**Results:** The proliferation of HT22 cells was significantly inhibited in the RT group, but was significantly preserved in the RT + MSC-CM group ( $P < 0.01$ ). Apoptosis was significantly higher in the RT group than in the RT+ MSC-CM group ( $P < 0.01$ ). MSC-CM decreased intracellular ROS and MDA content after irradiation ( $P < 0.01$ ). GSH level and SOD activity were higher in the RT + MSC-CM group than in the RT group, as was MMP ( $P < 0.01$ ). MSC-CM decreased expression of  $\gamma$ -H2AX, P53, Bax, and cleaved-caspase-3, but increased Bcl-2 expression ( $P < 0.01$ ).

<sup>1</sup> North China University of Science and Technology, Tangshan, Hebei Province, China

<sup>2</sup> Department of Orthopaedics, Tianjin Hospital, Tianjin, China

<sup>3</sup> Tianjin Key Laboratory of Food and Biotechnology, State Experimental and Training Centre of Food and Drug, School of Biotechnology and Food Science, Tianjin University of Commerce, Beichen, Tianjin, China

<sup>4</sup> Department of Hematology, Affiliated Hospital of North China University of Science and Technology, Tangshan, Hebei Province, China

<sup>5</sup> The Third Central Hospital of Tianjin, Hedong District, Tianjin, China

<sup>6</sup> Tianjin Key Laboratory of Extracorporeal Life Support for Critical Diseases, Tianjin, China

<sup>7</sup> Artificial Cell Engineering Technology Research Center, Tianjin, China

<sup>8</sup> Tianjin Institute of Hepatobiliary Disease, Tianjin, China

<sup>9</sup> Department of Anesthesiology, First Teaching Hospital of Tianjin University of Traditional Chinese Medicine, Tianjin, China

Received 22 July 2020; received revised 06 December 2020; accepted 07 December 2020

## Corresponding Authors:

Jing Zhang, The Third Central Hospital of Tianjin, Hedong District, Tianjin 300170, China.

Email: yadibaby1019@163.com

Qingling Qi, Department of Anesthesiology, First Teaching Hospital of Tianjin University of Traditional Chinese Medicine, Tianjin 300381, China.

Email: qiqinglingdr@163.com

Naiyao Chen, Department of Hematology, Affiliated Hospital of North China University of Science and Technology, Tangshan 063000, Hebei Province, China.

Email: nychenncmc@163.com



Creative Commons Non Commercial CC BY-NC: This article is distributed under the terms of the Creative Commons Attribution-NonCommercial 4.0 License (<https://creativecommons.org/licenses/by-nc/4.0/>) which permits non-commercial use, reproduction and distribution of the work without further permission provided the original work is attributed as specified on the SAGE and Open Access pages (<https://us.sagepub.com/en-us/nam/open-access-at-sage>).

**Conclusion:** MSC-CM attenuated radiation-induced hippocampal neuron cell line damage by alleviating oxidative stress and suppressing apoptosis.

### Keywords

mesenchymal stem cells, radiation, HT22 cells, oxidative stress, apoptosis, biomarker

## Introduction

Radiation treatment (RT) has become the predominant treatment for primary and secondary intracranial tumors, which are increasing in incidence.<sup>1</sup> However, radiation can damage the surrounding healthy brain tissue, inducing radiation-related cognitive dysfunction.<sup>2</sup> Radiation induces excessive production of reactive oxygen species (ROS) and neuroinflammation, which are important causes of neuronal loss.<sup>3</sup> Ionizing radiation produces free radicals by directly interacting with organic biomolecules, and also indirectly generates ROS such as  $H_2O_2$ ,  $O_2\bullet^-$ , and  $\bullet OH$  through indirect effects of ionization on intracellular water molecules.<sup>4</sup> Excessive ROS induced by RT not only destroy the nitrogenous bases, purines, pyrimidines and deoxyribose skeletons of DNA, but also damage mitochondrial DNA and proteins, potentially compromising mitochondrial function and inducing apoptosis.<sup>5</sup>

Mesenchymal stem cells (MSCs) possess self-renewal, differential proliferation, and multidirectional differentiation capacities. MSCs are easy to obtain, do not present ethical concerns, are easy to isolate and purify, and are not malignantly transformed.<sup>6</sup> In the context of neuroprotection, MSCs produce brain-derived neurotrophic factor (BDNF), vascular endothelial growth factor (VEGF), nerve growth factor (NGF), hepatocyte growth factor (HGF), transforming growth factor (TGF), and secreted product of tumor necrosis factor (TNF)-stimulated gene-6.<sup>7,8</sup> Our prior study demonstrated that in rats with traumatic brain injury, tail vein infusion of MSCs significantly increased expression of BDNF, VEGF, NGF and other proteins in the injured peri-cerebral cortex, decreased apoptosis, and significantly improved neurological function.<sup>9</sup> MSCs are speculated to promote nerve regeneration, which could be related to their paracrine effects in generating neurotrophic and growth factors. In fact, an increasing number of studies suggests that paracrine or metabolic factors play a leading role in the potential regenerative effects of MSCs.<sup>10</sup>

However, it is unclear whether MSCs can protect against radiation-induced brain injury. Therefore, the present study aimed to investigate the protective effects of MSC-CM against radiation-induced injury in a hippocampal neuronal cell line (HT22), and to elucidate the underlying mechanism of action. In particular, we investigated the effects of MSC-CM on ROS production and oxidative stress markers, as oxidative stress is a major cause of radiation-induced neuronal loss. We hypothesized that MSC-CM would protect against radiation-induced neuronal injury by attenuating radiation-induced oxidative stress and activating the neuroprotective PI3K/AKT pathway.

## Materials and Methods

### HT22 Culture

HT22 cells were purchased from Shanghai Saibaikang Biotechnology and cultured in Dulbecco's Modified Eagle's Medium (DMEM Gibco, Invitrogen, CA, USA) containing 10% fetal bovine serum (FBS, Gibco, Invitrogen, CA, USA) and incubated with 5%  $CO_2$  in a humidified atmosphere at 37°C.

### Preparation of MSC-CM

MSCs, obtained from the Affiliated Hospital of North China University of Technology, were cultured in minimum essential medium- $\alpha$  ( $\alpha$ -MEM, Gibco, Invitrogen, CA, USA) containing 10% FBS in a  $CO_2$  incubator. At approximately 80% confluency, cells were passaged using 0.05% trypsin and seeded in a new culture plate. The third passage of MSCs was seeded in a new culture plate at a concentration of  $1 \times 10^6$  cells/ml and cultured for 24 hours. Growth media was then replaced with serum-free  $\alpha$ -MEM medium for 48 h. The conditioned media was then transferred to a 15 ml centrifuge tube and centrifuged at  $5000 \times g$  for 10 mins at 4°C to remove cell debris, generating MSC-CM.

### Drug Preparation

To make a 1 M N-Acetylcysteine (NAC) stock solution, 1.63 g NAC was dissolved in 10 ml ultrapure water, filter-sterilized with a 0.22  $\mu m$  membrane, stored in the dark, and subsequently diluted to 5 mM before use. To prepare a 4 mM LY294002 stock solution, 5 mg LY294002 was dissolved in 4.07 ml DMSO, stored in the dark, and subsequently diluted to a 5  $\mu M$  working solution prior to use.

### Experimental Design

HT22 cells were divided into 6 experimental groups: Control: adding complete medium without irradiation; Simple radiation treatment (RT): adding complete medium and treating with 10 Gy X-ray irradiation; Radiation treatment + MSC-CM (RT+MSC-CM): Administration of MSC-CM after 10 Gy X-ray irradiation; Non-irradiated MSC-CM (MSC-CM): Administration of MSC-CM without irradiation; Radiation + NAC (RT+NAC): HT22 cells received 10 Gy X-ray irradiation after pretreatment with NAC. LY294002: After 10 Gy X-ray irradiation, MSC-CM containing the PI3 K inhibitor LY294002 was administered.

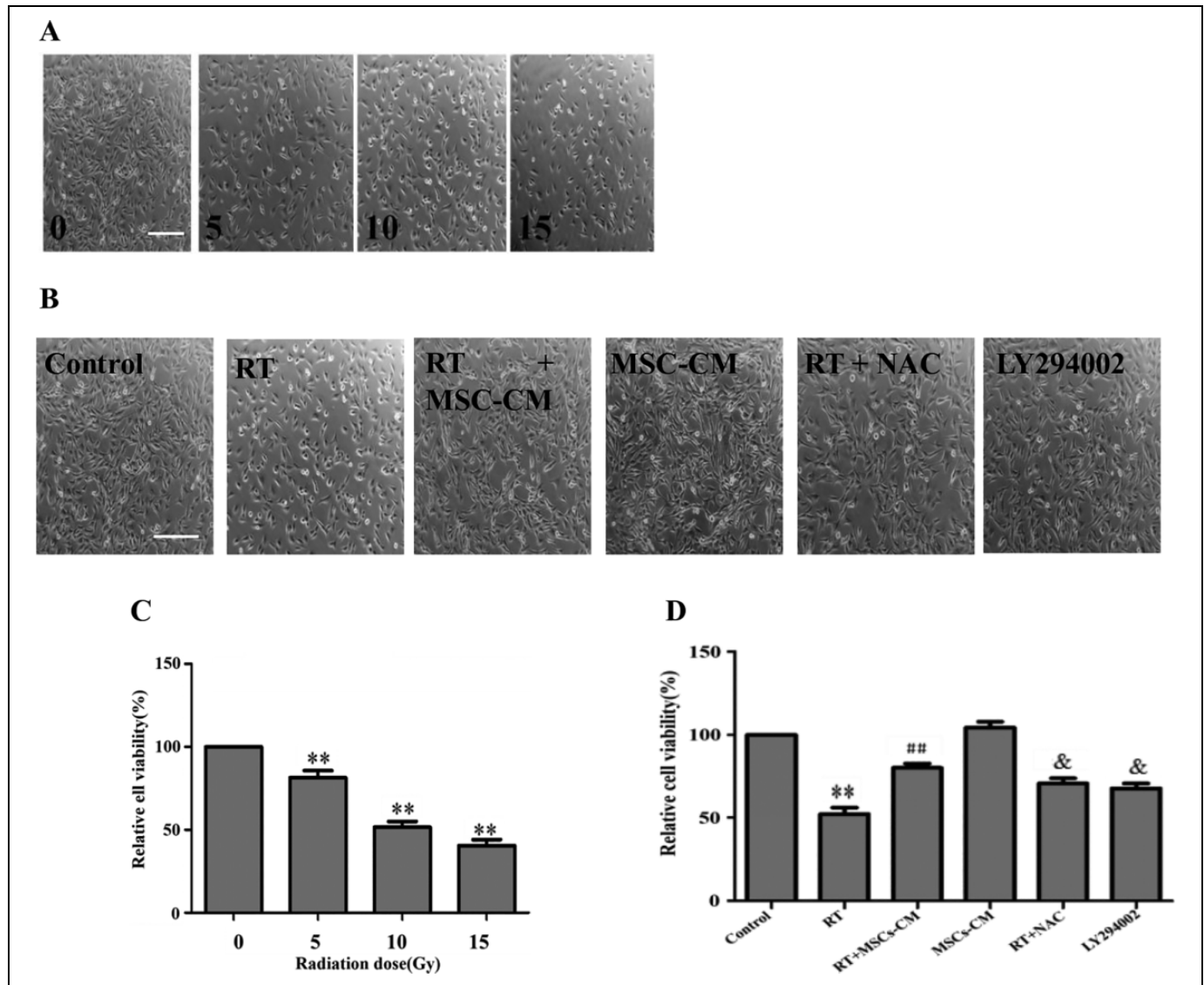


**Figure 1.** MSC-CM prevented radiation-induced suppression of HT22 proliferation. (A) Light microscopy (100 $\times$ ) shows the morphology of HT-22 cells exposed to the specified radiation doses. Scale bar, 100  $\mu$ M. (B) Light microscopy (100 $\times$ ) illustrates the morphology of HT-22 cells under the specified treatment conditions. (C) Effect of different radiation doses on HT22 cell viability. (D) Effect of different treatment conditions on HT-22 cell viability. Mean  $\pm$  SD. \*\* $P < 0.01$  vs Control; ## $P < 0.01$  vs RT; & $P < 0.05$  vs RT+MSC.

Irradiated HT22 cells received a single dose of 10 Gy at a dose rate of 6 Gy/min and 50 cm away from the irradiation source.

#### Analysis of Cells by Microscopy and CCK-8 Assay

HT-22 cells were irradiated with increasing doses of x-ray irradiation (0, 5, 10, and 15 Gy). To determine cell status and viability, microscopy and a CCK-8 assay were used. Five fields were observed with an inverted microscope (TE-2000 Nikon, Japan) and randomized to record changes in cell number and morphology. CCK-8 was added to each well and after further incubation for 1 h at 37 $^{\circ}$ C, the media were preserved for analysis. Absorbance was read at 450 nm to calculate the cell proliferation rate. At a radiation dose of 10 Gy, HT-22

proliferation was inhibited by approximately 50% (Figure 1). After administering the treatments described in the experimental design, changes in the number and morphology of the cells in each group was observed, and the proliferation rate was calculated.

#### Flow Cytometric Analysis

After treatment with RT and/or MSC-CM, cells were harvested by trypsinization and washed once with phosphate-buffered saline (PBS; pH 7.4). After centrifugation, cells were stained with annexin V and propidium iodide (PI) using the annexin V-FITC apoptosis detection kit (BD Biosciences, USA) according to the manufacturer's protocol.

### Measurement of MMP and ROS

For analysis of ROS and MMP, H<sub>2</sub>-DCFDA or JC-1, respectively, were added and incubated at 37°C for 15 min. Multiple viewing fields were photographed under a fluorescence microscope (TE-2000 Nikon, Japan).

### ELISA

After treatment, HT22 cells were cultured for 24 h and subsequently collected, washed twice with PBS, and disrupted by sonication. Total protein concentration was determined by the Bradford method, and GSH, MDA, and SOD levels were detected by ELISA. Each experiment was independently performed at least 3 times.

### Western Blotting

To measure protein levels of P/T-PI3 K, P/T-AKT,  $\gamma$ -H2AX, P/T-P53, Bax, Cleaved-Caspase-3, and Bcl-2, proteins were extracted from HT22 cells using radioimmunoprecipitation assay (RIPA) buffer. Samples were centrifuged at 12,000 rpm for 20 min at 4°C, and the supernatant was collected for protein analysis. Total protein concentration of each sample was determined with the BCA protein assay. Subsequently, 20  $\mu$ g protein of each sample was loaded onto a 12% sodium dodecyl sulfate gel, separated by electrophoresis and transferred to a polyvinylidene fluoride membrane. Membranes were blocked with 5% skim milk powder for 2 h at room temperature, and were then incubated with primary antibodies overnight at 4°C. After washing, membranes were incubated with secondary antibody for 1 h at room temperature. The signals on membranes were visualized by an enhanced chemiluminescence (ECL) western blotting detection kit (ZOMANBIO).  $\beta$ -actin was used as a loading control. All the experiments were repeated in triplicate.

### Statistical Analyses

All experiments described in the study were repeated at least 3 times. Statistical analysis was performed using SPSS statistical software, version 17.0. Results are presented as means  $\pm$  SEMs. A one-way analysis of variance (ANOVA) and repeated measures ANOVA were used for multivariate data analyses.  $P \leq 0.05$  was considered statistically significant.

## Results

### Optimal Radiation Dose Selection

Figure 1A shows cell morphology at 0, 5, 10, and 15 Gy radiation doses from left to right. As the radiation dose increased, cell density gradually decreased, cell bodies became rounded, and cell protrusions became shorter. After receiving different doses of radiation, the proliferation rate of HT-22 cells decreased in a dose-dependent manner (Figure 1C,  $P < 0.01$ ). The cell proliferation rate was approximately 50% at 10 Gy, and this dose was selected for subsequent studies.

### MSC-CM Protected HT22 Cells Against RT-Induced Cytotoxicity

As shown in Figure 1B and 1D, MSC-CM promoted cell proliferation and improved cell morphology and proliferation activity in HT-22 cells exposed to radiation.

### MSC-CM Inhibited ROS and MDA Accumulation and Increased GSH and SOD Activity

We hypothesized that MSC-CM would attenuate RT-induced increased production of ROS. ROS production was significantly higher in the RT group than in the control, but was significantly inhibited in the RT + MSC-CM group (Figure 2A). This was also the case for MDA levels (Figure 2B). SOD activity (Figure 2C) and GSH levels (Figure 2D) were lower in the RT group, but were significantly preserved in the RT+MSC-CM group.

### MSC-CM Attenuated Radiation-Induced Apoptosis by Improving MMP

Jc-1 is a fluorescent probe widely used to detect the MMP. Under normal physiological conditions when MMP is normal, JC-1 aggregates in the form of a polymer in the mitochondrial matrix, emitting red fluorescence. After radiation treatment, JC-1 accumulates in the form of a monomer into the patina, emitting green fluorescence, indicating disruption of the MMP. Therefore, green and red fluorescence intensity are indicative of cellular MMP.

Radiation decreased MMP in HT22 cells and promoted apoptosis. However, the MSC-CM partially restored MMP and decreased apoptosis in irradiated cells (Figure 3).

### Western Blotting

We examined the roles of signaling molecules in the protective effect of MSC-CM against radiation-induced neuronal death by investigating their activation (phosphorylation) using Western blotting.

### MSC-CM Treatment Activated PI3K/Akt Signaling

The primary function of phosphorylated PI3 K (P-PI3 K) is to phosphorylate AKT. Phosphorylated AKT (P-AKT) plays an important regulatory role in cell apoptosis, cell proliferation, angiogenesis, and other cellular processes and functions. PI3K-AKT signaling is a classic central nervous system protective pathway. Earlier studies showed that MSC-CM could activate PI3K/Akt signaling, which is regulated by phosphorylation. In the present study, we examined the roles of these signaling molecules in mediating radiation-induced neuronal death and the protective effect of MSC-CM in HT22 cells by measuring their activation (phosphorylation). With or without RT, 24 h treatment with MSC-CM significantly activated (phosphorylated) PI3K/AKT (Figure 4). We used a selective

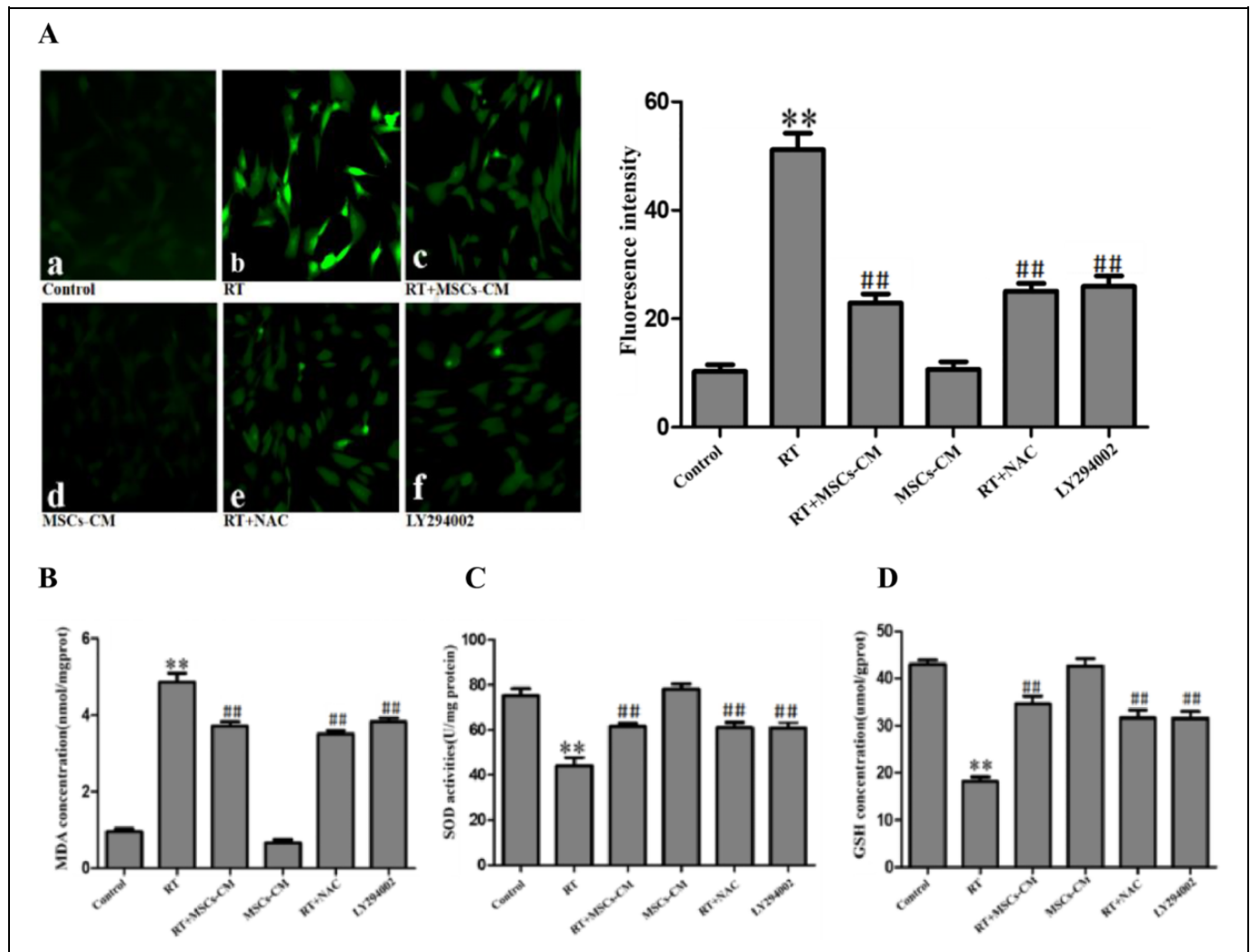


**Figure 2.** MSC-CM alleviated RT-induced oxidative stress. (A) Fluorescence microscopy analysis of intracellular ROS generation. (B) Colorimetric analysis of MDA levels. (C) SOD activity in the specified groups. (D) GSH levels in the specified groups. Mean  $\pm$  SD. \*\*P < 0.01 vs. Control and ##P < 0.01 vs. RT.

inhibitor of these signaling proteins (LY294002) to further investigate their functional roles in protection of HT22 cells from RT. When HT22 cells were cultured in MSC-CM with LY294002, the protective effects of MSC-CM were abrogated, as was activation of PI3K/AKT (Figure 4).

### MSC-CM Inhibited Apoptosis by Attenuating Radiation-Induced DNA Damage

Radiation induces apoptosis in part through ROS-mediated DNA damage. We next sought to determine the molecular mechanism of RT-induced HT22 apoptosis. Many pro- and anti-apoptotic proteins play well-established roles during apoptosis. Therefore, we determined whether classical mitochondria-associated pro- and anti-apoptotic proteins such as Bax and Bcl-2 were involved in RD-induced HT-22 apoptosis, and measured protein levels of cleaved Caspase-3, the effector caspase of the intrinsic apoptotic pathway.

In HT22 cells, both mitochondrial apoptotic mediators and the intrinsic apoptotic pathway were affected by RT and MSC-CM (Figure 4). Protein levels of P53, Bax,  $\gamma$ -H2AX and cleaved Caspase-3 were increased while Bcl-2 levels were decreased in irradiated cells (RT) relative to the control. These findings suggested that that RT promoted cell death by modulating both positive and negative regulators of apoptosis. Strikingly, these changes were reversed in irradiated cells treated with MSC-CM (RT+MSC-CM).

## Discussion

Radiation encephalopathy is a serious complication after radiotherapy targeting primary and metastatic brain tumors of the central nervous system. Radiation-induced brain injury (RIBI) leads to neuronal apoptosis, decreased neurogenesis, and subsequent cognitive impairment. Radiation-induced cognitive

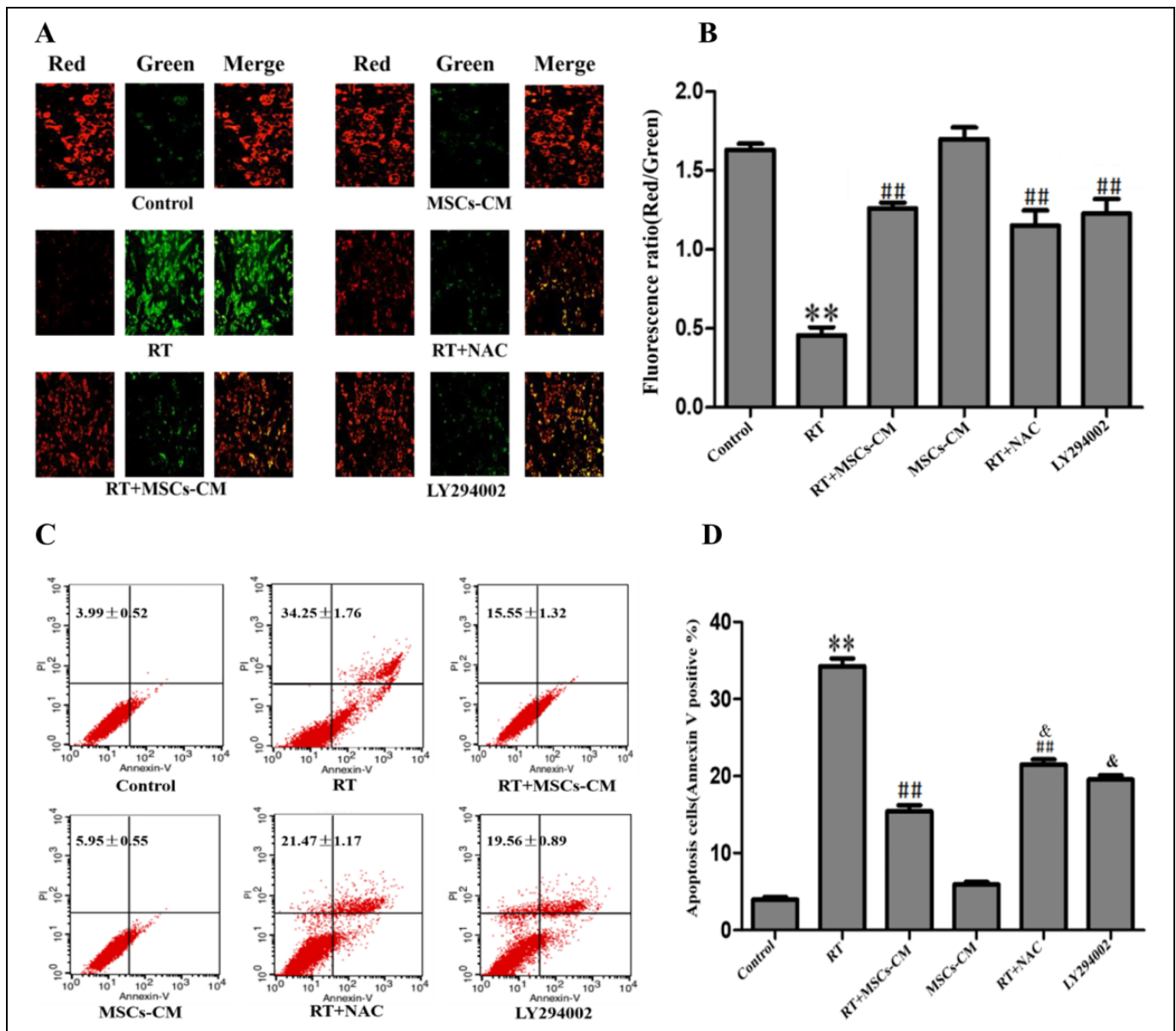


**Figure 3.** Effect of MSC-CM on MMP and apoptosis in irradiated HT-22 cells. (A-B) MMP of HT-22 cells under the specified conditions. Mean  $\pm$  SD. (C-D) Apoptosis rates of HT-22 cells under the specified conditions. Mean  $\pm$  SD. vs Control \*\* $P < 0.01$  Vs Control; ## $P < 0.01$  vs RT; & $P < 0.05$  vs RT+MSC.

dysfunction is a significant concern worldwide, and multiple studies have attempted to address this unmet clinical need.<sup>11</sup>

Oxidative stress has long been recognized as a leading cause of acute and chronic radiation damage. In many cell lines, intracellular ROS continue to increase after irradiation.<sup>12,13</sup> Increased ROS react with polysaturated fatty acids to form the lipid peroxide MDA, leading to membrane instability and lipid peroxide generation. Therefore, cellular MDA content changes reflect the overall degree of lipid peroxidation, and also indirectly reflect the degree of cell damage.<sup>14</sup> The present study also found that radiation promoted production of ROS and MDA in HT22 cells, further supporting its role in increased ROS generation and oxidative stress. The

body's antioxidant system includes both enzymatic and non-enzymatic protective mechanisms. SOD as an important antioxidant enzyme that can decompose  $O_2\bullet^-$  into  $H_2O$  and  $O_2$ . It is thought to be the first line of defense against  $O_2\bullet^-$  increases in cells and tissues. It is also considered as the main line of defense to prevent damage caused by increased ROS and lipid peroxidation.<sup>15</sup> Additionally, GSH can react with glutamate peroxidase to protect the body from oxidative damage inflicted by endogenous ROS.<sup>16</sup> The present study demonstrated that MSC-CM and NAC decreased ROS and MDA production and increased SOD activity and GSH levels in the irradiated HT22 cells, indicating that it can protect against radiation induced oxidative stress.

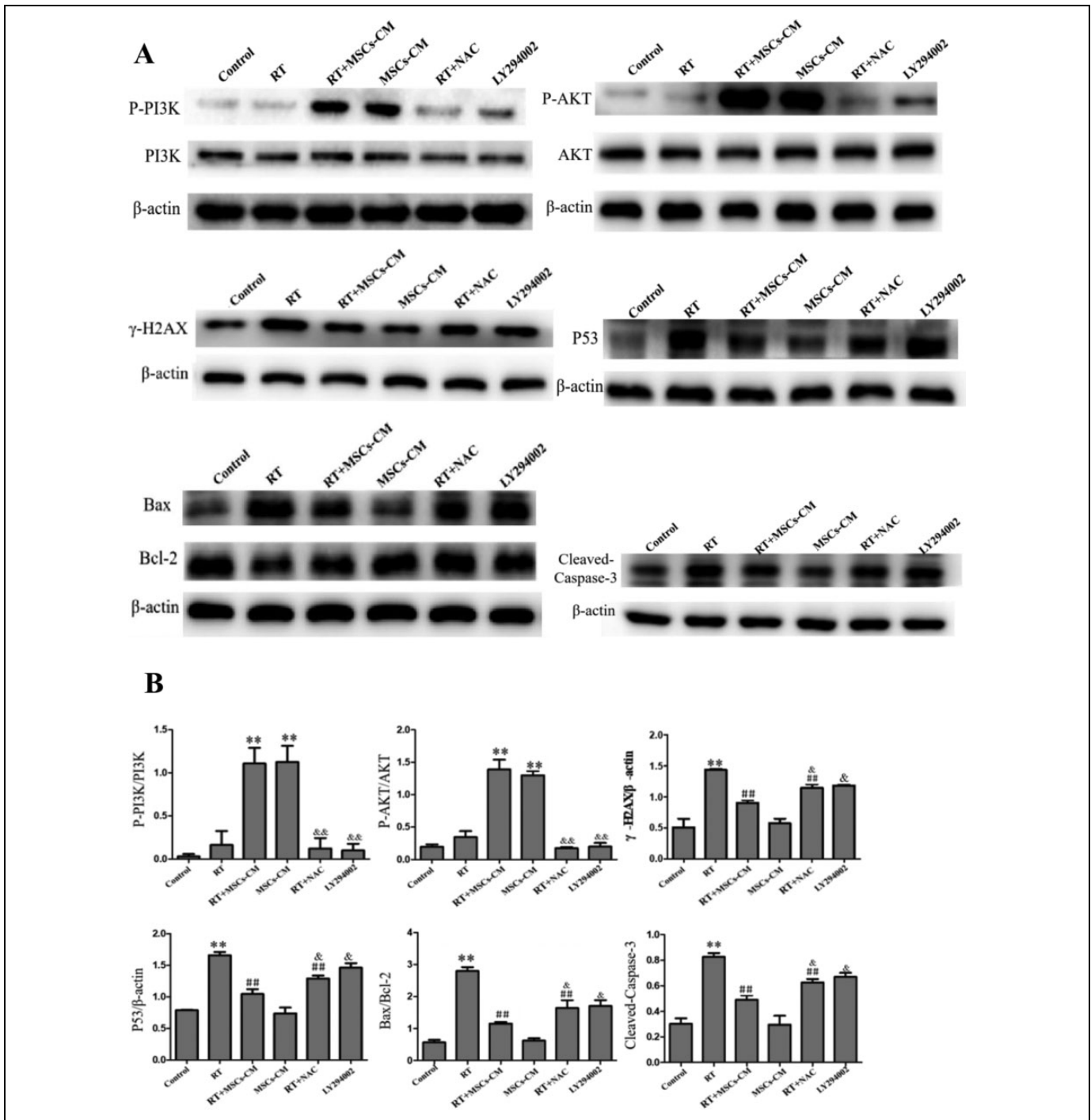


**Figure 4.** X-Ray irradiation and MSC-CM oppositely regulated pro- and anti-apoptotic mediators in HT-22 cells. (A) Western blot assay of P-PI3K, P-AKT,  $\gamma$ -H2AX, p53, Bax, Bcl-2, and cleaved caspase-3. (B) Bar diagrams showing relative protein expression from Western blot analysis. Data were normalized with  $\beta$ -actin expression. Values are expressed as Mean  $\pm$  SD. \*\*P < 0.01 vs. Control, ##P < 0.01 vs. RT and &P < 0.05 vs. RT+MSC-CM.

Post-radiation hippocampal dysfunction is closely associated with radiation-induced oxidative stress and mitochondrial dysfunction.<sup>17</sup> In recent years, a large number of studies have demonstrated that when cells undergo apoptosis in various contexts, the MMP declines. ROS can also cause apoptosis and decrease the MMP, so it may contribute to the observed effects

of RT on MMP.<sup>12</sup> Our experiments found that radiation caused mitochondrial damage, as demonstrated by decreased MMP in HT22 cells after radiation. In turn, decreased MMP further exacerbated mitochondrial dysfunction, further increasing ROS production and perpetuating a vicious cycle by which ROS production continually increases after irradiation, further

damaging organelles and ultimately inducing apoptosis.<sup>5,18</sup> The present study suggested that MSC-CM can increase the MMP in neurons exposed to RT, which could potentially alleviate radiation-induced apoptosis.

PI3K is necessary for neural tube and hippocampal neuron differentiation.<sup>19,20</sup> Therefore, in a wide variety of neuronal cells, activation of the PI3K-AKT pathway has been strongly implicated in cell survival and proliferation.<sup>21</sup> To determine how MSC-CM-mediated PI3K/AKT activation increased the antioxidant capacity of irradiated HT22 cells, we sought to determine the involvement of the PI3K/AKT signaling pathways. PI3K/AKT was phosphorylated (activated) after MSC-CM treatment. To determine if the protective effects of MSC-CM were dependent on PI3K/AKT activity, a parallel experiment using the PI3K inhibitor LY294002 was performed. Pretreatment of cells with LY294002 suppressed MSC-CM activation of the PI3K/AKT pathway, and abrogated the anti-apoptotic and antioxidant effects of MSC-CM in HT-22 cells subjected to RT. Together, these findings suggested that MSC-CM attenuated radiation-induced apoptosis by activating the PI3K/AKT pathway.

Ionizing radiation directly inflicts DNA damage by energy deposition, and indirectly inflicts DNA damage through ionization of water molecules. ROS can cause DNA damage, including DNA strand break, DNA site mutation, DNA strand distortion and proto-Oncogene and tumor inhibitor gene mutation, by attacking proteins and DNA.<sup>22</sup> DNA double strand breaks (DSBs) are one of the primary causes of DNA damage. If not rapidly repaired, DSBs act as strong inducers of cell death.<sup>23</sup>  $\gamma$ -H2AX is formed by phosphorylation of the serine at position 139 on histone H2AX after DSBs. For DSBs induced by radiation or oxidative damage,  $\gamma$ -H2AX increases in a dose-dependent manner. Therefore,  $\gamma$ -H2AX is widely used to detect cellular DSBs.<sup>24</sup> On the basis of Western blot findings, our results indicated that MSC-CM treatment decreased expression of the DSB-related factor  $\gamma$ -H2AX.

Previous studies have demonstrated that oxidative stress can not only directly induce apoptosis, but can also indirectly promote apoptosis by activating P53.<sup>25</sup> P53 is a well-known stress-responsive protein, and is closely tied to neurodegenerative diseases such as Parkinson's Disease (PD) and Alzheimer's disease (AD). P53 plays a key regulatory role in a variety of cellular processes, including cell cycle control, DNA damage repair, apoptosis and senescence.<sup>26-28</sup> Radiation upregulates p53 expression. Upon stimulation, p53 can initiate apoptotic processes by activation of the mitochondrial pathway. This mitochondrial pathway includes inactivation of the anti-apoptotic protein Bcl-2, translocation of the apoptotic protein Bax to mitochondrial membrane pores, and release of cytochrome c to the cytosol. Release of cytochrome c initiates caspase 3 cleavage that ultimately induces apoptosis.<sup>29</sup>

The Bcl-2 family is an important protein family for regulating and controlling apoptosis, and is primarily involved in mitochondrial pathway-mediated apoptosis.<sup>30</sup> The ratio of the apoptotic protein Bax to the anti-apoptotic protein Bcl-2 is an important determinant of apoptosis, and can ultimately activate the caspase

cleavage cascade.<sup>31</sup> Caspases are the most important enzymes involved in apoptosis. After activation, caspases hydrolyze important structural and functional proteins of cells, ultimately leading to apoptosis.<sup>32</sup> In the present study, Western blotting demonstrated that expression of the apoptotic proteins P53, Bax, and cleaved caspase-3 increased and the expression of the anti-apoptotic protein Bcl-2 decreased after RT, suggesting that radiation induced apoptosis through these mechanisms in HT22 cells. Both MSC-CM and NAC reversed these changes, indicating that MSC-CM and NAC can alleviate radiation-induced neuronal apoptosis, and potentially be used as neuroprotectants in the context of radiotherapy.

## Conclusions

The present study evaluated the pro-survival and anti-apoptotic effects of MSC-CM in the context of neuronal radiation damage. In an effort to determine the mechanism by which MSC-CM decreased apoptosis in irradiated HT-22 cells, we studied the effect of MSC-CM on ROS production, DNA damage, and expression of apoptotic and anti-apoptotic proteins. Our findings revealed a neuroprotective role for MSC-CM in this context, suggesting MSC-CM could be a potential treatment for radiation-related cognitive dysfunction. However, the detailed mechanisms will need to be investigated in a future study.

## Acknowledgments

The authors thank Medical Laboratory of North China University of Science and Technology for laboratory environment support. We also thank Hong Xu at the Medical Laboratory of North China University of Science and Technology for his technical help.

## Author Contribution

Yue Huang and Xiaolong Mei equally contributed to this work.

## Declaration of Conflicting Interests

The author(s) declared no potential conflicts of interest with respect to the research, authorship, and/or publication of this article.

## Funding

The author(s) disclosed receipt of the following financial support for the research, authorship, and/or publication of this article: The study was supported by Provincial Government Funded Clinical Medicine Excellent Talents Training Projective in 2014, Hebei Provincial Health Department (NO. H2013209253). This study was also supported by the CAMS Innovation Fund for Medical Science (2017-I2M-1-016), Tianjin Science and Technology Project (19ZXDBSY00100), National Natural Science Foundation incubation project of Tianjin Third Central Hospital and Tianjin Key Laboratory of in vitro life support for severe diseases (2019YNR5), and the Key R&D Program of Shandong Province (2019GSF107056).

## ORCID iD

Yue Huang  <https://orcid.org/0000-0001-8962-305X>

## References

- Bae YS, Oh H, Rhee SG, Yoo YD. Regulation of reactive oxygen species generation in cell signaling. *Mol Cells*. 2011;32(6):491-509. doi:10.1007/s10059-011-0276-3
- Ren F, Wang K, Zhang T, Jiang J, Nice EC, Huang C. New insights into redox regulation of stem cell self-renewal and differentiation. *Biochim Biophys Acta*. 2015;1850(8):1518-1526. doi:10.1016/j.bbagen.2015.02.017
- Rola R, Zou Y, Huang TT, et al. Lack of extra-cellular superoxide dismutase (EC-SOD) in the microenvironment impacts radiation-induced changes in neurogenesis. *Free Radic Biol Med*. 2007;42(8):1133-1145. doi:10.1016/j.freeradbiomed.2007.01.020
- Losada-Barreiro S, Bravo-Diaz C. Free radicals and polyphenols: the redox chemistry of neurodegenerative diseases. *Eur J Med Chem*. 2017;133:379-402. doi:10.1016/j.ejmech.2017.03.061
- Stepien KM, Heaton R, Rankin S, et al. Evidence of oxidative stress and secondary mitochondrial dysfunction in metabolic and non-metabolic disorders. *J Clin Med*. 2017;6(7):71. doi:10.3390/jcm6070071
- Obtulowicz P, Lech W, Strojek L, Sarnowska A, Domanska-Janik K. Induction of endothelial phenotype from Wharton's jelly-derived MSCs and comparison of their vasoprotective and neuroprotective potential with primary WJ-MSCs in CA1 hippocampal region ex vivo. *Cell Transplant*. 2016;25(4):715-727. doi:10.3727/096368915X690369
- Madriral M, Rao KS, Riordan NH. A review of therapeutic effects of mesenchymal stem cell secretions and induction of secretory modification by different culture methods. *J Transl Med*. 2014;11(12):260. doi:10.1186/s12967-014-0260-8
- Guo ZY, Sun X, Xu XL, Zhao Q, Peng J, Wang Y. Human umbilical cord mesenchymal stem cells promote peripheral nerve repair via paracrine mechanisms. *Neural Regen Res*. 2015;10(4):651-658. doi:10.4103/1673-5374.155442
- Zhao J, Chen N, Shen N, et al. Transplantation of human umbilical cord blood mesenchymal stem cells to treat a rat model of traumatic brain injury. *Neural Regen Res*. 2012;7(10):741-748.
- Ferreira JR, Teixeira GQ, Santos SG, Barbosa MA, Almeida-Porada G, Gonçalves RM. Mesenchymal stromal cell secretome: influencing therapeutic potential by cellular pre-conditioning. *Front Immunol*. 2018;4(9):2837. doi:10.3389/fimmu.2018.02837. eCollection 2018
- Gerstenecker A, Meneses K, Duff K, Fiveash JB, Marson DC, Triebel KL. Cognitive predictors of understanding treatment decisions in patients with newly diagnosed brain metastasis. *Cancer*. 2015;121(12):2013-2019.
- Mukherjee SB, Das M, Sudhandiran G, Shaha C. Increase in cytosolic Ca<sup>2+</sup> levels through the activation of non-selective cation channels induced by oxidative stress causes mitochondrial depolarization leading to apoptosis-like death in Leishmania donovani promastigotes. *J Biol Chem*. 2002;277(27):24717-24727.
- Trachootham D, Alexandre J, Huang P. Targeting cancer cells by ROS-mediated mechanisms: a radical therapeutic approach? *Nat Rev Drug Discov*. 2009;8(7):579-591.
- Valko M, Rhodes CJ, Moncol J, Izakovic M, Mazur M. Free radicals, metals and antioxidants in oxidative stress-induced cancer. *Chem Biol Interact*. 2006;160(1):1-40. doi:10.1016/j.cbi.2005.12.009
- Ebadi M, Govitrapong P, Sharma S, et al. Ubiquinone (coenzyme q10) and mitochondria in oxidative stress of Parkinson's disease. *Biol Signals Recept*. 2001;10(3-4):224-253.
- Huang WM, Xing W, Li DH, Liu YD. The role of glutathione metabolism in tolerance of tobacco BY-2 suspension cells to microcystin-RR. *Bull Environ Contam Toxicol*. 2008;80(3):215-219.
- Son Y, Yang M, Wang H, Moon C. Hippocampal dysfunctions caused by cranial irradiation: a review of the experimental evidence. *Brain Behav Immun*. 2015;45:287-296.
- Brand MD. Mitochondrial generation of superoxide and hydrogen peroxide as the source of mitochondrial redox signaling. *Free Radic Biol Med*. 2016;100:14-31. doi:10.1016/j.freeradbiomed.2016.04.001
- Peltier J, O'Neill A, Schaffer DV. PI3K/Akt and CREB regulate adult neural hippocampal progenitor proliferation and differentiation. *Dev Neurobiol*. 2007;67(10):1348-1361.
- Fishwick KJ, Li RA, Halley P, Deng P, Storey KG. Initiation of neuronal differentiation requires PI3-kinase/TOR signalling in the vertebrate neural tube. *Dev Biol*. 2010;338(2):215-225.
- Yu Y, Wu X, Pu J, et al. Lycium barbarum polysaccharide protects against oxygen glucose deprivation/reoxygenation-induced apoptosis and autophagic cell death via the PI3K/Akt/mTOR signaling pathway in primary cultured hippocampal neurons. *Biochem Biophys Res Commun*. 2018;495(1):1187-1194.
- Meiral B, Bugni JM, Green SL, et al. DNA damage induced by chronic inflammation contributes to colon carcinogenesis in mice. *J Clin Invest*. 2008;118(7):2516-2525.
- Roos WP, Kaina B. DNA damage-induced cell death by apoptosis. *Trends Mol Med*. 2006;12(9):440-450.
- Luczak MW, Zhitkovich A. Monoubiquitinated  $\gamma$ -H2AX: abundant product and specific biomarker for non-apoptotic DNA double-strand breaks. *Toxicol Appl Pharm*. 2018;355:238-246.
- Liu B, Chen Y, St Clair DK. ROS and p53: a versatile partnership. *Free Radic Biol Med*. 2008;44(8):1529-1535.
- Lanni C, Racchi M, Memo M, Govoni S, Uberti D. P53 at the crossroads between cancer and neurodegeneration. *Free Radic Biol Med*. 2012;52(9):1727-1733.
- Elias J, Dimitrio L, Clairambault J, Natalini R. The p53 protein and its molecular network: modelling a missing link between DNA damage and cell fate. *Biochim Biophys Acta*. 2014;1844(1 pt B):232-247.
- Kracikova M, Akiri G, George A, Sachidanandam R, Aaronson SA. A threshold mechanism mediates p53 cell fate decision between growth arrest and apoptosis. *Cell Death Differ*. 2013;20(4):576-588.

29. Gupta S, Kass G E N, Szegezdi E, Joseph B. The mitochondrial death pathway: a promising therapeutic target in diseases. *J Cell Mol Med.* 2010;13(6):1004-1033.
30. Pohl SO, Agostino M, Dharmarajan A, Pervaiz S. Crosstalk between cellular redox state and the anti-apoptotic protein Bcl-2. *Antioxid Redox Signal.* 2018;29(13):1215-1236. doi:10.1089/ars.2017.7414
31. Liu QS, Deng R, Li S, et al. Ellagic acid protects against neuron damage in ischemic stroke through regulating the ratio of Bcl-2/Bax expression. *Appl Physiol Nutr Metab.* 2017;42(8):855-860. doi:10.1139/apnm-2016-0651
32. Cullen SP, Martin SJ. Caspase activation pathways: some recent progress. *Cell Death Differ.* 2009;16(7):935-938.